Biomedical Signal Processing and Control 40 (2018) 335–342

Contents lists available at ScienceDirect

Biomedical Signal Processing and Control

journal homepage: www.elsevier.com/locate/bspc

Research Paper

Surface EMG based continuous estimation of human lower limb joint angles by using deep belief networks

Jiangcheng Chen[a,b,*], Xiaodong Zhang[a], Yu Cheng[b], Ning Xi[b]

[a] School of Mechanical Engineering, Xi'an Jiaotong University, Shannxi 710049, PR China
[b] Department of Industrial and Manufacturing Systems Engineering, The University of Hong Kong, Pokfulam, Hong Kong Special Administrative Region

ARTICLE INFO

Article history:
Received 7 December 2016
Received in revised form 6 August 2017
Accepted 7 October 2017
Available online 16 October 2017

Keywords:
Multichannel surface EMG
Joint angle estimation
Deep belief networks
Principal components analysis
Restricted boltzmann machines
Back propagation network

ABSTRACT

Surface electromyography (EMG) signals have been widely used in locomotion studies and human-machine interface applications. In this paper, a regression model which relates the multichannel surface EMG signals to human lower limb flexion/extension (FE) joint angles is constructed. In the experimental paradigm, three dimensional trajectories of 16 external markers on the human lower limbs were recorded by optical motion capture system and surface EMG signals from 10 muscles directly concerned with the lower limb motion were recorded synchronously. With the raw data, the joint angles of hip, knee and ankle were calculated accurately and the time series of intensity for surface EMG signals were extracted. Then, a deep belief networks (DBN) that consists of restricted Boltzmann machines (RBM) was built, by which the multi-channel processed surface EMG signals were encoded in low dimensional space and the optimal features were extracted. Finally, a back propagation (BP) neural network was used to map the optimal surface EMG features to the FE joint angles. The results show that, the features extracted from multichannel surface EMG signals using DBN method proposed in this paper outperform principal components analysis (PCA), and the root mean square error (RMSE) between the estimated joint angles and calculated ones during human walking is reduced by about 50%. The proposed model is expected to develop human-machine interaction interface to achieve continuous bioelectric control and to improve motion stability between human and machine, especially for lower limb wearable intelligent equipment.

1. Introduction

The new-class of intelligent equipment, such as rehabilitation robots, power-assisted robots, and intelligent prosthetics, require human-machine interaction and collaboration is the focus of research in the field of robotics [1–3]. With the development of bio-information technology, EEG, EMG, and other biological signals have been widely used to develop interface for man-machine systems. Surface EMG signal is the recording of muscle electrical activity and is much stronger than EEG signal. By performing a signal processing procedure on the raw surface EMG signals, muscle activity and body movement information can be acquired. Therefore, engineers use surface EMG to develop feasible interface for man-machine systems. The most notably application is as a souse of control for the Human Assisted Limb (HAL) exoskeleton [4].

In recent years, surface EMG signals have been extensively used to extract human motion information in two ways. For the first way, researchers use surface EMG signals to recognize different motion modes of human limbs. In this way, higher recognition rate and more motion modes are the two goals and feature extraction methods and classification algorithms are the research focus [5–9]. However, only a limited number of motion modes can be identified from surface EMG signals and the recognition results are only used as a switch signal for the robot. As a result, the smoothness of movement of robot and the coordination between human and robot are affected greatly. By contrast, the second way in which surface EMG signals are used to continue estimate the motion variables can achieve smooth motion control. Many methods have been proposed to build the relationship between the surface EMG signals and movement variables. For example, a forward biomechanical model is constructed and calibrated to calculate the joint torques by using surface EMG signals [10]. Artificial neural networks [11–13] and polynomial fitting [14] are also used to map the surface EMG signals to joint angles or joint torques. Although these methods have been applied to specific applications successfully, they still suffer some problems. For example, the forward biomechanical

* Corresponding author at: School of Mechanical Engineering, Xi'an Jiaotong University, No. 28, Xianning West Road, Xi'an, Shannxi 710049, PR China.
E-mail addresses: jiangcheng.0502@163.com (J. Chen), xdzhang@mail.xjtu.edu.cn (X. Zhang).

https://doi.org/10.1016/j.bspc.2017.10.002
1746-8094/

model includes many physiological parameters which have a vast difference between individuals and a calibration is required for a specific subject. Comparing with the biomechanical model method, the regression methods, such as artificial neural network, show the merits of simple and quick. Moreover, the estimation accuracy can be improved if more available channels of surface EMG signal are used as the input.

For the regression methods, feature extraction and selection contributes significantly to the learning efficiency and estimation accuracy of the regression model. How to extract the optimal features which is continuous, robust and non-redundant from multichannel surface EMG signals has become the key issue. In the previous work, principal component analysis (PCA) is often used to obtain an optimal feature vector from multichannel surface EMG signals [6,15,16]. However, PCA is a linear dimensionality reduction algorithm and cannot extract the nonlinear structure components which hide in high dimensional dataset. So PCA has limitations for the surface EMG signals which have high and strong nonlinear characteristics. In order to automatically learn the complex structure components from high dimensional dataset and achieve a dimension reduction, Hinton et al. [17] proposed an efficient and fast learning algorithm for the deep neural networks which has many hidden layers and uses the trained network to convert high dimensional data to lower dimensional codes. For such a multilayer network, the output of each layer contains all the information of the input data and can be seen as a new code of the input data in a new space. The dimensionality of input vectors can be reduced by using a multilayer network with a small central layer to reconstruct them. Most importantly, it has been proved that this network can reveal the nonlinear structure hide in high dimensional data because of multiple levels of non-linear operations.

The aim of this work is to build the regression model which relates the multichannel surface EMG signals to human lower limb joint angles in order to develop a more natural human-machine interface. Specifically, in this research, a deep belief networks is built to extract the optimal feature vectors that has low dimensionality from multichannel surface EMG signals and a back propagation network is used to map the optimal feature vectors to the lower limb joint angles. To validate the effectiveness of the methods proposed in this paper, experiments have been conducted and the results showed that higher estimation accuracy was obtained comparing to the traditional methods.

This paper includes four sections in total and these sections are arranged as follows: Section 2 talks about the proposed method, to be more specific, it introduces about the acquisition of gait kinematics data and surface EMG data as well as the joint angles calculation, surface EMG data processing, and back propagation network construction. Section 3 presents the experimental results followed by a discussion. Finally, Section 4 concludes the paper.

2. Experimental and method

2.1. Data acquisition

Gait is a basic movement for human lower limbs and estimating the joint angles of lower limbs under human walking is the main goal of this work. The dataset used in this paper were collected in the scenarios of human walking. Six able-bodied people were selected in this study, with age ranging from 24 to 30 (mean ± S.D.: 26 ± 2.2 years). Body weight ranges from 57 to 74 kg (62.6 ± 3.7 kg), and body height ranges from 166 to 180 cm (170.6 ± 3.6 cm). All subjects were required to complete walking on flat ground with speeds of 0.8, 1.0, 1.2 m/s and transition speed from 0.8 to 1.2 m/s, separately. Each trial was repeated 3 times. During each trial, the surface EMG signals from ten muscles which relate to the movements of right leg were collected with a wireless surface EMG collection device (MyoMove–EOW, Shanghai Ncc Electronic Company Limited, P.R. China). The sample rate is 1200 Hz and the muscles selected were biceps femoris (BF), semitendinosus (ST), vastus medialis (VM), vastus lateralis (VL), rectus femoris (RF), sartorius (SR), medial gastrocnemius (MG), lateral gastrocnemius (LG), anterior tibialis (AT), and soleus (SL). The disposable circular electrodes with a diameter 10 mm were placed according to the guideline of SENIAM [18] and the locations of electrodes are shown in Fig. 1. Meanwhile, the kinematics data of 16 motion capture markers placed on the surface of lower limbs were collected using a 10-camera optical motion capture system (VICON, Oxford Metrics Limited, UK); the sample rate is 100 Hz and the position numbers and names of external marker positions are described in Table 1. The motion capture system, VICON, mainly consists of MX-cameras, MX-Giganet, and host PC with NEXUS software. The MX-Giganet, which connects the host PC and MX-cameras, provides interface between VICON and EMG system and allows the kinematics and EMG data to be recorded synchronously.

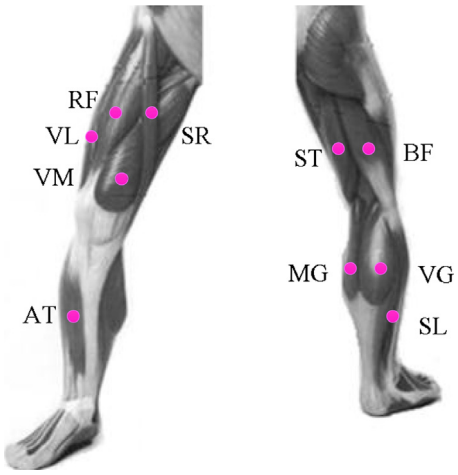

Fig. 1. Locations of electrodes in surface EMG measurement.

Table 1
Position numbers and the corresponding names of external marker positions for motion capture.

No.	name	No.	name
1	Left anterior superior iliac spines	9	Right lateral knee
2	Right anterior superior iliac spines	10	Right medial knee
3	Left posterior superior iliac spine	11	Right lateral ankle
4	Right posterior superior iliac spine	12	Right medial ankle
5	Left lateral knee	13	Left metatarsal head
6	Left medial knee	14	Left heel
7	Left lateral ankle	15	Right metatarsal head
8	Left medial ankle	16	Right heel

2.2. Markers data processing

Correct calculation of joint angles is a prerequisite for building their relationship to the surface EMG signals. The joint angles can be computed by using the trajectories of markers in this work and the calculation procedure is as follows:

The first step is to determine the positions of the joint centers and segment centers of gravity by using the data of makers. The knee and ankle centers can be approximated by the midpoints of the two external markers attached beside the corresponding joint. For the hip center determination, the method proposed by Camomilla et al. [19] could be used. Taking the midpoint of the left and right anterior superior iliac spines (ASIS) as the base point, the local reference frame of the pelvis is set up, as shown in Fig. 2. Then

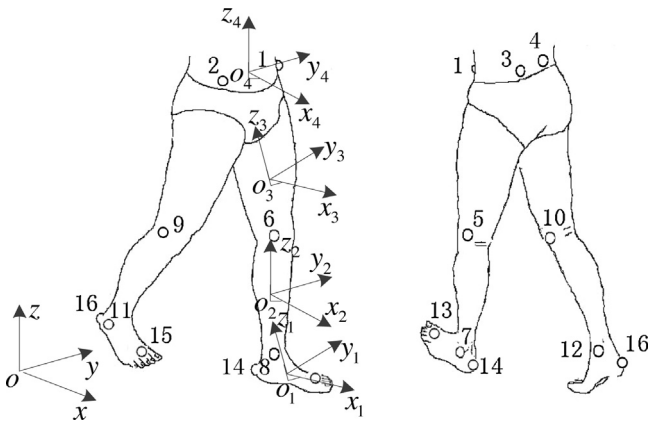

Fig. 2. The motion capture marker placement as well as the reference frames.

the position vector of hip center in the pelvis reference frame is determined based on the following linear regression equation [20]

$$\begin{cases} x = -0.24\mathrm{P_d} - 9.9 \\ y = -0.30\mathrm{P_w} - 10.9 \\ z = 0.33\mathrm{P_w} + 7.3 \end{cases} \tag{1}$$

where $\mathrm{P_d}$ represents the pelvic depth. It refers to the distance between the midpoint of two ASIS and the midpoint of two posterior superior iliac spines (PSIS); $\mathrm{P_w}$ represents the pelvic width, which refers to the distance between two ASIS (units: mm). After obtaining the positions of joint centers, the centers of gravity locations can be derived [21]:

$$P_{\mathrm{Thigh.CG}} = P_{\mathrm{hip}} + 0.39(P_{\mathrm{knee}} - P_{\mathrm{hip}}) \tag{2}$$

$$P_{\mathrm{Calf.CG}} = P_{\mathrm{knee}} + 0.42(P_{\mathrm{ankle}} - P_{\mathrm{knee}}) \tag{3}$$

$$P_{\mathrm{Foot.CG}} = P_{\mathrm{heel}} + 0.44(P_{\mathrm{toe}} - P_{\mathrm{heel}}) \tag{4}$$

where $\boldsymbol{p}_{\mathrm{hip}}$, $\boldsymbol{p}_{\mathrm{knee}}$, and $\boldsymbol{p}_{\mathrm{ankle}}$ indicate the joint center positions of hip, knee, and ankle, respectively. $\boldsymbol{p}_{\mathrm{knee}}$ and $\boldsymbol{p}_{\mathrm{ankle}}$ indicate the positions of metatarsal head and heel, respectively.

The second step is to generate the segment reference frames embedded at the segment centers of gravity. For example, the unit vector triad for reference frame of thigh can be generated as

$$k_3 = \frac{p_{\mathrm{hip}} - p_{\mathrm{knee}}}{|p_{\mathrm{hip}} - p_{\mathrm{knee}}|} \tag{5}$$

$$i_3 = \frac{(p_{\mathrm{knee}} - p_{\mathrm{hip}}) \times (p_5 - p_{\mathrm{hip}})}{|(p_{\mathrm{knee}} - p_{\mathrm{hip}}) \times (p_5 - p_{\mathrm{hip}})|} \tag{6}$$

$$j_3 = k_3 \times i_3 \tag{7}$$

Similarly, the unit vector triads of reference frames for pelvis, left calf, and left foot can be generated, as shown in Fig. 2.

The third step is to determine the angles of joint rotation. As we all know, each joint connects two body segments together and the joint angles can be defined as a rotation of one segment relative to another one. In this paper, the two segments linked by one joint are called proximal segment and distal segment. Taking the knee joint as an example, they are the thigh and calf respectively. Moreover, considering that the orientation of a segment can be described by its reference frame, the joint angle can be defined as a rotation of the distal frame to the proximal one. Make a convention apply to all joints: set $\boldsymbol{j}_{\mathrm{proximal}}$ as the flexion/extension axis and α is the flexion/extension angle, set $\boldsymbol{k}_{\mathrm{distal}}$ as the internal/external rotation axis and $\boldsymbol{\gamma}$ is the internal/external rotation angle, set $\boldsymbol{l}_{\mathrm{joint}}$ as the abduction/adduction axis and is the abduction/adduction angle, of which the vector $\boldsymbol{l}_{\mathrm{joint}}$ is defined as

$$l_{joint} = \frac{j_{\mathrm{proximal}} \times k_{\mathrm{distal}}}{|j_{\mathrm{proximal}} \times k_{\mathrm{distal}}|} \tag{8}$$

Based on the above definition and take the knee as an example, the joint angles can be calculated as follows

$$\alpha_{knee} = \sin^{-1}[l_{\mathrm{knee}} \cdot k_3] \tag{9}$$

$$\beta_{\mathrm{knee}} = -\sin^{-1}[j_3 \cdot k_2] \tag{10}$$

$$\gamma_{\mathrm{knee}} = \sin^{-1}[l_{\mathrm{knee}} \cdot j_2] \tag{11}$$

2.3. Surface EMG signal processing

In this study, the processing of surface EMG signals is divided into two steps. Firstly, the time series of intensity for each surface EMG signal are calculated which constitute 10 dimensional feature vectors. Then, these initial feature vectors are sent into a deep belief network which outputs 3 dimensional vectors. The detailed processes of the two steps are listed below:

2.3.1. Extraction of surface EMG intensity

There are mainly three types of features in analysis of the surface EMG signal. They are time domain, frequency domain and time-frequency domain. Among the three types, features in time domain are quick and easily implemented because they do not need any transformation. So the surface intensity extracted in time domain is used in this study. The raw surface EMG signals are a mixture of noise signals and original surface EMG signals. The noise signals include inherent noises which come from industrial frequency interference and movement artifacts noises. They are unnecessary and should be removed. A notch filter with 50 Hz (industrial frequency) and a zero-lag fourth-order recursive Butterworth filter with 20 Hz can be applied to all of the raw surface EMG signals. After removing the noises, the signals are full-wave rectified and subsampled with 100 Hz frequency to be consistent with joint angle signals to remove the noise. After above processing, the time series of intensity for all channels of surface EMG signal could be extracted by applying a Butterworth low-pass filter with a 4 Hz cut-off frequency to the signals. Finally, all the time series of intensity constitute the initial 10 dimensional feature vectors for 10 channels of surface EMG signals.

2.3.2. Feature dimension reduction by using DBN

In order to obtain the optimal feature vectors from the initial 10 dimensional feature vectors, a deep belief network (DBN) with a small central layer is built and implemented. DBN is a kind of network organized in deep architecture and shows higher modeling capacity than shallow architectures. However, for decades, it was believed that training is very difficult for such multilayer neural networks. The past practice suggested that the gradient-based optimization is powerless for such deep neural networks since it often gets stuck in poor solutions due to the lack of good initialization methods. Fortunately, Hinton et al. [17] proposed an efficient layer-by-layer learning algorithm for DBNs and solved this problem well. A DBN can be trained by two steps that called layer-wise pre-training and fine-tuning, respectively. The layer- wise pre-training step is to training a stack of RBMs recursively and quickly which results in a set of initial network parameters. In the fine-tuning step, the RBMs are unfolded to produce the DBN with the same parameters and on which the gradient-based optimization algorithm is performed further to minimize the discrepancy between the input data and its output data.

The building block of the DBN is called restricted Boltzmann machines (RBM). An RBM is a two-layer, undirected, and energy

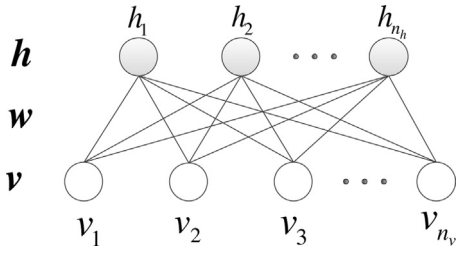

Fig. 3. Schematic diagram of RBM architecture.

based model in which the visible units in the first layer represent observations, and the visible units are connected to the hidden units which represent the features in the second layer [22]. There are interaction terms between a visible unit and a hidden unit, but not between units in the same layer. The graphical model of an RBM model is shown in Fig. 3. In this figure, v, $\boldsymbol{w}$, and $\boldsymbol{h}$ represent the visible unit data, the weight parameters, and the hidden unit data respectively. In order to make it easily accessible to readers, the concept of RBM and its training method are introduced in detail below.

In a binary RBM model, a joint configuration, $(v, \boldsymbol{h})$ of the hidden and visible units has an energy determined by the model parameters and can be defined as

$$\mathrm{E}_\delta(v, h) = -\sum_{i=1}^{n_v}\sum_{j=1}^{n_h} w_{ij} v_i h_j - \sum_{i=1}^{n_v} b_i v_i - \sum_{j=1}^{n_h} a_j h_j \tag{12}$$

where $\boldsymbol{\delta} = (\boldsymbol{w}, \boldsymbol{a}, \boldsymbol{b})$ is a parameter matrix for the RBM model and w_{ij} is the interaction weight connecting the visible unit v_i and the hidden unit h_j, a_i and b_i are the constant offsets, and n_v and n_h are the number of units corresponding to visible and hidden layers respectively. Through the energy function of (12), the RBM model assigns a probability to every possible visible-hidden vector pairs $(v, \boldsymbol{h})$ and can be calculated as

$$\mathrm{P}_\delta(v, h) = e^{-E_\delta(v,h)} / \sum_{v,h} e^{-E_\delta(v,h)} \tag{13}$$

As a consequence of no interaction terms between either visible units or hidden units, the conditional distribution $P_{\boldsymbol{\delta}}(\boldsymbol{h}\,|\boldsymbol{v})$ and $P_{\boldsymbol{\delta}}(\boldsymbol{v}\,|\boldsymbol{h})$ can be given by

$$P_\delta(h_j = 1|v) = f\left(b_j + \sum_{i=1}^{n_v} w_{j,i} v_i\right) \tag{14}$$

$$P_\delta(\mathrm{v}_i = 1|h) = f\left(a_\mathrm{i} + \sum_{j=1}^{n_h} w_{j,i} v_j\right) \tag{15}$$

where $f(\cdot)$is the sigmoid activation function.

For a practical issue, we would be more interested in the marginal probability of observed vectors (e.g., the initial feature vectors in this study). By marginalizing over the space of hidden vectors, the marginal probability that the network assigns to a input vector can be calculated and described as

$$P_\delta(v) = \sum_h e^{-E_\delta(v,h)} / \sum_{v,h} e^{-E_\delta(v,h)} \tag{16}$$

In fact, the task of training the RBM is to maximize the marginal probability by adjusting the model parameters [23]. The derivative of the log marginal probability of input vector with respect to a weight, visible unit offset, and hidden unit offset are

$$\frac{\partial \log(P_\delta(v))}{\partial w_{ij}} = \langle v_i h_j \rangle_{\mathrm{data}} - < v_i h_j >_{\mathrm{model}} \tag{17}$$

$$\frac{\partial \log(P_\delta(v))}{\partial a_i} = \langle v_i \rangle_{\mathrm{data}} - < v_i >_{\mathrm{model}} \tag{18}$$

$$\frac{\partial \log(P_\delta(v))}{\partial b_j} = \langle h_j \rangle_{\mathrm{data}} - < h_j >_{\mathrm{model}} \tag{19}$$

where the angle brackets indicate the expectations under the distribution specified in the subscript. This leads to update rules for raising the marginal probability of input data

$$\Delta w_{ij} = \varepsilon \left(\langle v_i h_j \rangle_{\mathrm{data}} - < v_i h_j >_{\mathrm{model}}\right) \tag{20}$$

$$\Delta a_i = \varepsilon \left(\langle v_i \rangle_{\mathrm{data}} - < v_i >_{\mathrm{model}}\right) \tag{21}$$

$$\Delta b_j = \varepsilon \left(\langle h_j \rangle_{\mathrm{data}} - < h_j >_{\mathrm{model}}\right) \tag{22}$$

where ε is the learning rate. For Eq. (20), it is very easy to compute the term of $< v_i h_j >_{\mathrm{data}}$ which is the expectation with respect to the training data distribution. However, it is much more difficult to get an unbiased sample that defined by the model and difficult to compute the term of $< v_i h_j >_{\mathrm{model}}$. It requires extensive iterations of alternating Gibbs sampling which takes a long time to get an exactly results [24]. So the contrastive divergence (CD) approximation of gradient is used to update the weights [25]. The process is as follows: initialize the visible unit states using a random training vector and compute the hidden unit states using Eq. (14), and then update the states of all the visible units using Eq. (15). The updated visible unit states are a reconstruction of the training vector. And then, use Eq. (14) to compute the hidden units from the reconstruction data. Finally, compute the $< v_i h_j >_{\mathrm{recon}}$ using reconstruction data and replace the term of $< v_i h_j >_{\mathrm{model}}$. Although this learning rule is an approximation to the gradient, it works well in discovering data feature in practice.

With the unsupervised learning algorithm for an RBM that presented above, the training of a DBN can be implemented. As mentioned above, the first step is the layer-wise pre-training, which is to train a stack of RBMs (as shown in Fig. 4(a)). The training of the stacked RBMs is as follows: the training data $\boldsymbol{X}_\mathrm{O}$ (initial feature vectors of surface EMG) are fed into RBM-1 to update its weights and offsets until the number of epochs is reached. Then, the parameters of RBM-1 are fixed and the outputs are treated as the input data for training the upper-level RBM, which refers to as RBM-2, and go forward layer by layer, until the top level RBM-m which has a lower dimensionality output compared with RBM-1.

After training the stacked RBMs, the RBMs are unfolded to produce the DBN with the same model parameters, as shown in Fig. 4(b). In the DBN, each layer of the DBN is a feature detector and optimizing the parameters of all the layers is needed in order to improve its performance. So the fine-tuning step whose goal is to minimize the discrepancy between the input data $\boldsymbol{X}_\mathrm{O}$ and the output data $\boldsymbol{X}_\mathrm{R}$ of the network is carried out. Because a set of good initial values for the DBN parameters have been learned during the unsupervised pre-training step, back propagation algorithm can be used efficiently to fine-tune the parameters for optimal reconstruction. Finally, the lower dimensionality codes of central layer of the DBN can be used as the optimal feature vectors $\boldsymbol{Y}$ that with respect to the initial feature vectors of surface EMG.

In this study, in order to reduce the dimensionality of initial feature matrix of surface EMG, a DBN which has 9 layers was constructed and the numbers of units for each layer were 10, 18, 12, 6, 3, 6, 12, 18, and 10 respectively. The codes of central layer which has 3 units ($m = 3$) were extracted and were used as the optimal feature vectors of surface EMG for each trial. It must explain that the number of units for central layer of the DBN was determined by using PCA that which was used to reduce the dimensionality of feature matrix in advance. In the case of using PCA, the first three of principal components were capable of describing 85% of the initial surface EMG feature matrix.

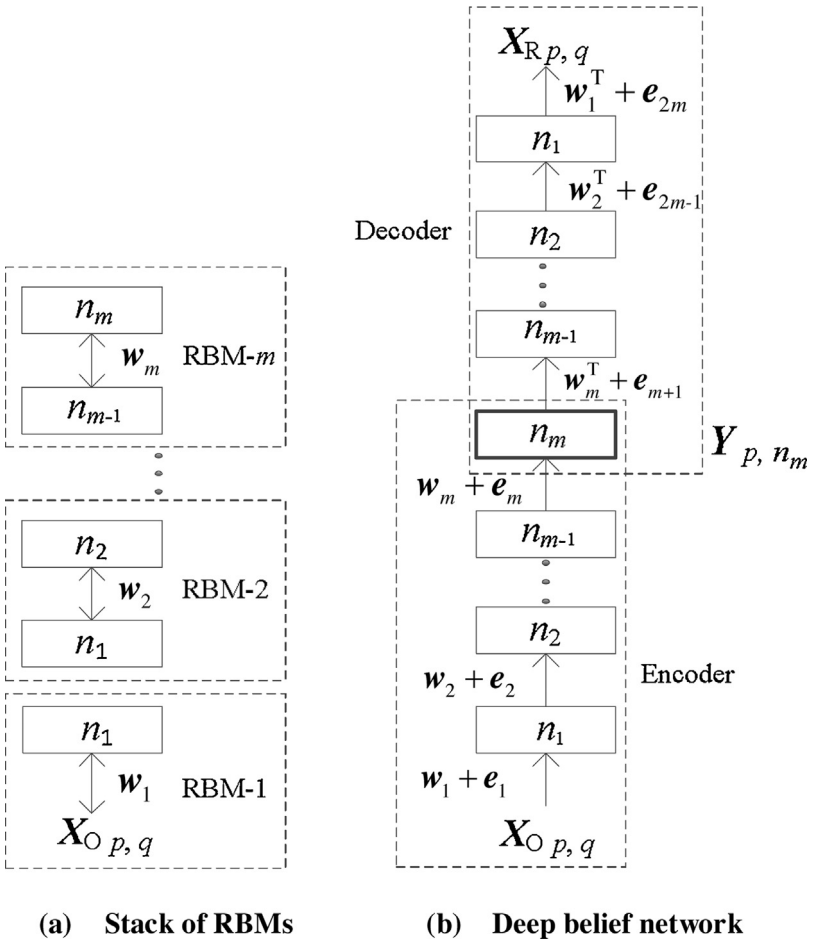

Fig. 4. The typical topological structure of deep belief networks.

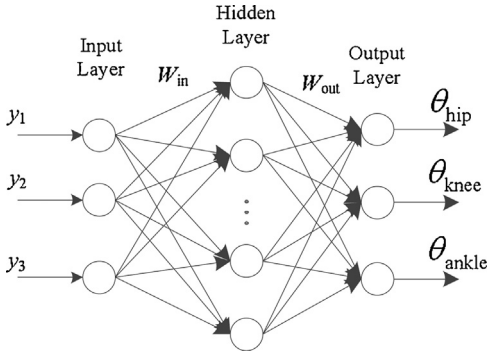

Fig. 5. The topological structure of the BP network.

2.4. BP network for angle estimation

In general, the relationships between each muscle activity and joint angles are highly nonlinear and difficult to be described with conventional approach [11–13]. Therefore, after obtaining the optimal feature vectors of surface EMG, a three layer BP neural network can be constructed and used to map the feature vectors to the FE joint angles and the topological structure is shown in Fig. 5. The input layer of the BP neural network consists of three nodes which represent three optimal feature vectors of surface EMG that generated by DBN. The input vector is represented by $\boldsymbol{Y}=[y_1, y_2, y_3]$. The output layer of the BP neural network consists of three nodes which predict the angles of lower limb joints rotation. The output vector is represented by $\tilde{\boldsymbol{\theta}}=[\tilde{\theta}_{\text{hip}}, \tilde{\theta}_{\text{knee}}, \tilde{\theta}_{\text{ankle}}]$ and they are FE angles. Only angles in the sagittal plane are estimated in this work considering that many wearable lower limb exoskeleton robots only have drivers in this plane. Besides, the number of hidden units is 12. Linear purelin function and tansig function can be selected as the transmission functions for the units in the output layer and the units in the hidden layer respectively. As a result, the output of the BP neural network can be calculated by

$$\dot{\boldsymbol{\theta}} = \boldsymbol{W}_{\text{out}}\left[\frac{2}{1+e^{-2(\boldsymbol{W}_{\text{in}}\boldsymbol{y}+\boldsymbol{b}_{\text{in}})}}-1\right]+\boldsymbol{b}_{\text{out}} \tag{22}$$

where $\boldsymbol{W}_{\text{in}}$ is the matrix consists of weights of the hidden layer, $\boldsymbol{W}_{\text{out}}$ is the matrix consists of weights of the output layer, and $\boldsymbol{b}_{\text{in}}$ and $\boldsymbol{b}_{\text{out}}$ are the threshold vectors.

Once the structure of the BP neural network is determined, the calculated target joint angle vectors and the optimal feature vectors can be used as the training data. In order to describe the estimation precision quantitatively, root mean square error (RMSE) η and the cross-correlation coefficient ρ between estimated and calculated joint angle values are used and can be calculated as (the formulas are suitable for any joint)

$$\eta = \sqrt{\frac{\sum_{i=1}^{N}(\tilde{\theta}_i-\theta_i)^2}{N}} \tag{23}$$

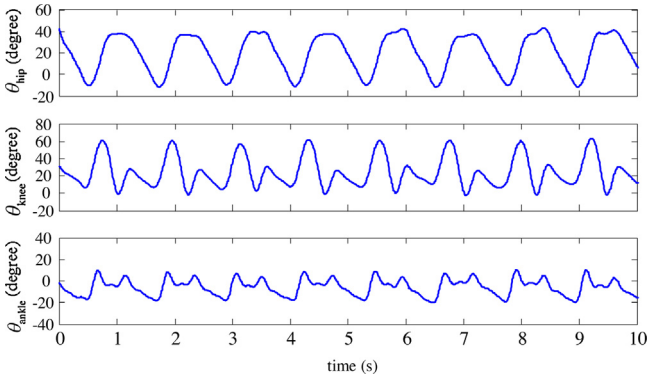

Fig. 6. The angle curves for one subject in one walking trail.

$$\rho = \frac{\sum_{i=1}^{N}(\tilde{\theta}_i - \bar{\tilde{\theta}})(\theta_i - \bar{\theta})}{\sqrt{\sum_{i=1}^{N}(\tilde{\theta}_i - \bar{\tilde{\theta}})^2}\sqrt{\sum_{i=1}^{N}(\theta_i - \bar{\theta})^2}} \tag{24}$$

where $\bar{\tilde{\theta}}$ is the mean value of the estimated joint angles, $\bar{\theta}$ is the mean value of the target joint angles, and N represents the number of value points.

3. Results and discussion

From six healthy subjects, 72 groups of raw data for different speed walking trials were collected in total. The joint angles were calculated across 12 trails for each subject with the method presented in Section 2.2 and the surface EMG intensity was also calculated across 10 channels (ch-1 ∼ ch-10) of raw surface EMG signals for each trial with the method presented in Section 2.3. At the same time, the 10 sets of time series of intensity constituted the initial feature matrix for each trail. Finally, all the calculated data were divided into two parts, and 30 groups of data were used as training data while the rest groups were served as testing data. Each subject provides 5 groups of data (one group from each uniform speed and two groups from transition speed) for the training data. Therefore, the training data cover all subjects and all walking speeds.

Fig. 6 shows the angle curves of one of the subjects in one walking trail. From the figure, we can find that the range of hip joint FE angle is from −20 to 40°, the range of knee joint FE angle is from 0 to 80°, and the range of ankle joint FE angle is from −30 to 20°. These ranges agree with the work by Schwartz [26]. In addition, the trend of the angle curves under walking is very close to the previous work [27].

Fig. 7 presents the comparison between the input data and output data from the trained DBN for one trial. In the figure, the blue lines indicate the input data (initial feature data) while the red lines indicate the output data (reconstruction data). It can be found that the DBN shows the perfect reconstruction ability as the discrepancy between the input data and the output data is small. By performing statistical analysis on all the data in this trial, the RMSE between the original data and reconstruction data is about 0.053 and it suggests that the reconstruction data retain vast majority information of original data after transforming for many times in the network. In other words, the codes of each layer can be used as a new feature vectors for the initial input data.

With the trained DBN, the time series of intensity of surface EMG in the groups of testing set were re-encoded. Fig. 8 shows a new three dimensional codes for the 10 channels of surface EMG signals

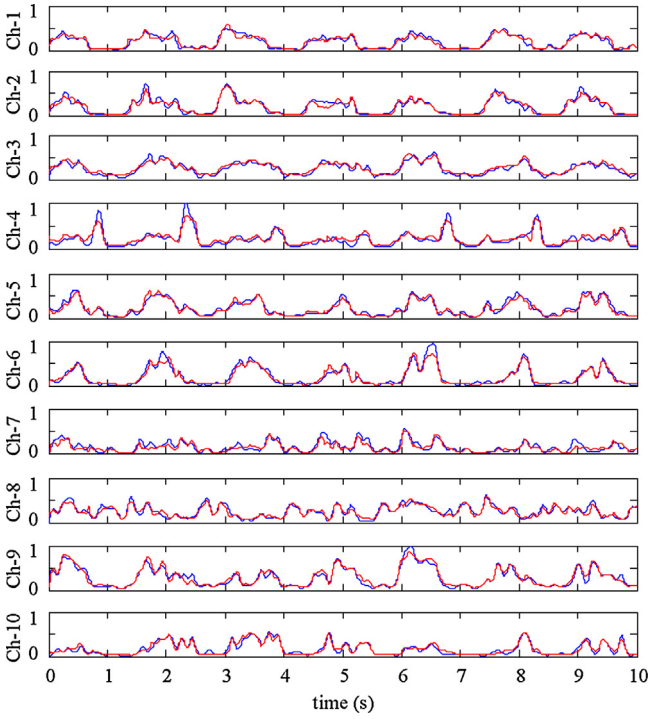

Fig. 7. The comparison between the input data and output data from the trained DBN for one trial (blue lines indicate the input data of DBN, red lines indicate the output data of DBN). (For interpretation of the references to colour in this figure legend, the reader is referred to the web version of this article.)

collected in one trial in which the walking speed was about 1.0 m/s. In order to make a comparison, the codes encoded by using PCA method and the codes encoded by using DBN method are presented in Fig. 8a and b respectively. Especially in the case of PCA method, the three principal components are capable of describing 86.7% of the total variance. In the data acquisition experiments, there are small variations between gait cycles in one trial as the subject was required to walk with almost the same speed. There are several gait cycles in 10 s and we can find that all the curves in Fig. 8b show a good periodicity and repeatability. However, the curves in Fig. 8a have poor periodicity and repeatability, especially for the third principle components. There is no doubt that this will affect the joint angle estimation precision. The result suggests that the DBN method is outperformed PCA method in extracting optimal feature vectors for multichannel surface EMG signals. The features extracted by DBN method are more stable.

With the new three dimensional codes of surface EMG signals and the trained BP neural network, the FE joint angles were estimated. The three dimensional codes from PCA and DBN were all used to estimate the joint angles. Fig. 9 illustrates the FE angle estimation result for one trial. In the figure, the black lines represent the calculated angles, the blue lines represent the estimation angles by using PCA method, and the red lines represent the estimation angles by using DBN method. This result shows the ability of proposed DBN method to accurately estimate lower limb FE joint angles during walking. Although there is greater variation in the shape of the angles, especially for the FE ankle angles, the BP model is still able to estimate the FE ankle angles ($\eta = 2.11°$ and $\rho = 0.97$) with the new three dimensional codes from DBN. And in the case of FE ankle angle estimation, the RMSE η and cross-correlation coefficient ρ are 4.32° and 0.80 respectively by using PCA method. Therefore, comparing with the estimation result by using PCA method, the DBN method shows better performance in capturing the shape of angle curve.

To validate the effectiveness of the proposed method further, statistical analysis was implemented and the results are presented

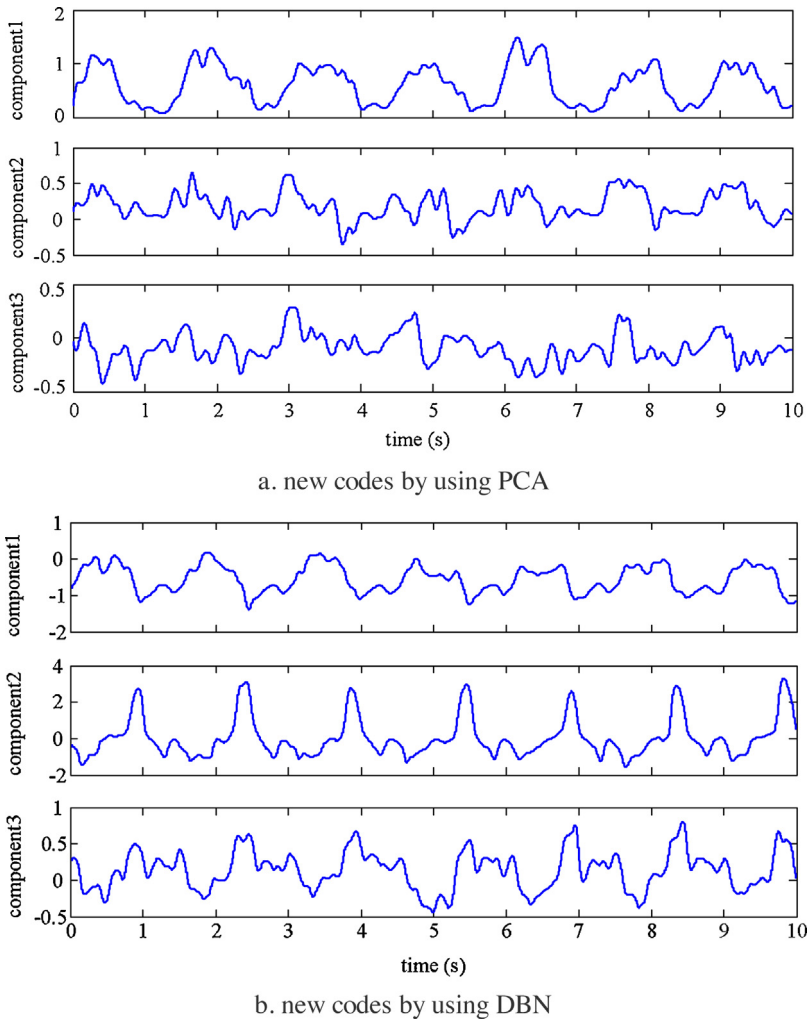

Fig. 8. The new three dimensional codes for multi-channel surface EMG signals in one trial.

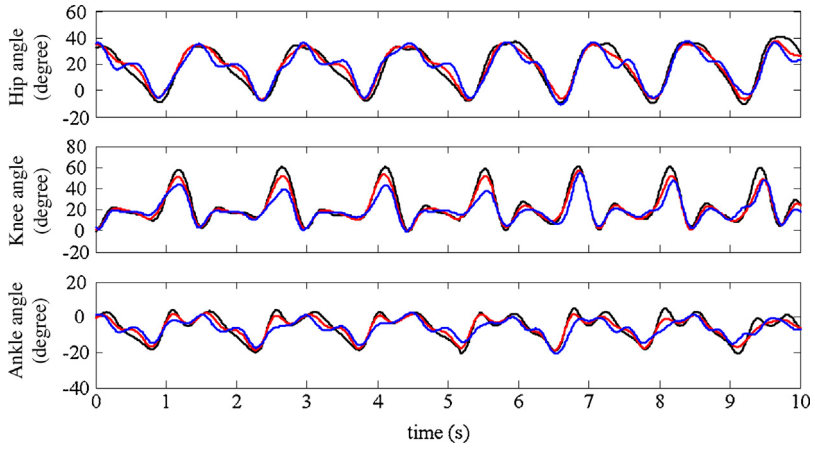

Fig. 9. The estimation result for human lower limb FE joint angles under walking for one subject. (Black lines indicate the calculated FE joint angles, blue lines indicate the estimated angles by using PCA method, and red lines indicate the estimated angles by using DBN method). (For interpretation of the references to colour in this figure legend, the reader is referred to the web version of this article.)

in Table 2. The estimation results of 30 trials anticipated in the statistical analysis and the performance indicators are RMSE η and cross-correlation coefficient ρ. From the table we can get the information that the errors of angle estimation for each joint by DBN method are lower than PCA while the cross-correlation coefficients are higher. On the whole, by utilizing the features learned by DBN, the RMSE between the estimated joint angles and calculated ones during human walking can be reduced by nearly 50% compared with PCA method.

All the above results are based on normal gait dataset from healthy people and shows a good performance. However, sometimes we may develop surface EMG based control interface for the

Table 2
FE joint angles estimation root mean square error η and the cross-correlation coefficient ρ under different walking speed for six able-bodied individuals by using DBN and PCA methods.

θ	DBN		PCA	
	η/degree	ρ	η/degree	ρ
θ_{hip}	3.58 ± 0.67	0.96 ± 0.05	6.22 ± 1.67	0.92 ± 0.06
θ_{knee}	3.96 ± 0.69	0.97 ± 0.04	8.11 ± 2.02	0.92 ± 0.07
θ_{ankle}	2.45 ± 0.57	0.95 ± 0.03	4.65 ± 1.32	0.86 ± 0.05

rehabilitation robot which is used to improving the gait of patients with neurological or musculoskeletal diseases, such as the people suffering from spinal cord injury (SCI). In this situation, the gait data recorded will be different and additional measures should be taken while the method proposed in this paper is applied. For the patients who only suffer one damaged side, the surface from the healthy side can be used as control signal due to symmetry of human lower limbs. In this case our method can be used directly. For the patients with a disease in both sides, the raw data should be collected from the patients under the gait guided by physiotherapist and a retraining of our model is required. In the research conducted by Zhang et al. [11], gait data from four SCI patients was recoded under the movements of passive treadmill exercises and the dataset was used to train a BP network which maps the surface EMG intensity to lower limb FE joint angles. Their results shows a good performance. Although we haven't verified our method with abnormal gait data, we believe the possible impact could be overcome.

4. Conclusions

This paper presents a continue FE angle estimation method for human lower limb joints in walking by using multichannel surface EMG signals. In this implementation, the joint angle calculation method for hip, knee and ankle based on optical motion capture system is applied firstly. Then, in view of the nonlinear characteristics of surface EMG single and the redundant information in multichannel signals, a nonlinear dimensionality reduction method based on DBN which constitutes of RBMs is presented. Finally, BP neural network is structured and trained to relate the optimal feature vectors and the calculated joint angles. All the proposed methods are validated by experiment data collected from six healthy subjects. In our further work, we will collect more data that cover wider range of tasks, such as running, jumping, and so on, to calibrate the regression model and make the model more generalized. Meanwhile, we will try to apply our method for patients with neurological or musculoskeletal diseases. The proposed strategy is expected to develop human-machine interaction interface to achieve continuous bioelectric control and for the improvement of motion stability between human and machine, especially for lower limb wearable intelligent equipment.

Acknowledgments

The authors are very grateful for the research support from China's National Natural Science Fund (No. 91420301).

References

[1] W. Meng, Q. Liu, Z. Zhou, et al., Recent development of mechanisms and control strategies for robot-assisted lower limb rehabilitation, Mechatronics 31 (2015) 132–145.
[2] R.A.R.C. Gopura, D.S.V. Bandara, Kazuo Kiguchi, et al., Developments in hardware systems of active upper-limb exoskeleton robots: a review, Rob. Auton. Syst. 75 (2016) 203–220.
[3] C. Cipriani, C. Antfolk, C. Balkenius, et al., A novel concept for a prosthetic hand with a bidirectional interface: a feasibility study, IEEE Trans. Biomed. Eng. 56 (11) (2009) 2739–2743.
[4] H. Kawamoto, S. Kanbe, Y. Sankai, Power assist method for HAL-3 estimating operator's intention based on motion information, Processing of the 2003 IEEE International Workshop on Robot and Human Interactive Communication (2003) 67–72.
[5] A. Phinyomark, F. Quaine, S. Charbonnier, et al., Feature extraction of the first difference of EMG time series for EMG pattern recognition, Comput. Meth. Prog. Biomed. 117 (2) (2014) 247–256.
[6] A.C. Tsai, J.J. Luh, T.T. Lin, A novel STFT-ranking feature of multi-channel EMG for motion pattern recognition, Expert Syst. Appl. 42 (7) (2015) 3327–3341.
[7] P. McCool, L. Petropoulakis, J.J. Soraghan, et al., Improved pattern recognition classification accuracy for surface myoelectric signals using spectral enhancement, Biomed. Signal Process. Control 18 (2015) 61–68.
[8] R. Lauer, B. Smith, R. Betz, Application of a neuro-fuzzy network for gait event detection using electromyography in the child with cerebral palsy, IEEE Trans. Biomed. Eng. 52 (9) (2005) 1532–1540.
[9] I. Mesa, A. Rubio, I. Tubia, Channel and feature selection for a surface electromyographic pattern recognition task, Expert Syst. Appl. 41 (11) (2014) 5190–5200.
[10] D.G. Lloyd, T.F. Besier, An EMG-driven musculoskeletal model to estimate muscle forces and knee joint moments in vivo, J. Biomech. 36 (2003) 765–776.
[11] F. Zhang, P.F. Li, Z.G. Hou, et al., sEMG-based continuous estimation of joint angles of human legs by using BP neural network, Neurocomputing 78 (1) (2012) 139–148.
[12] M.M. Ardestani, X. Zhang, L. Wang, et al., Human lower extremity joint moment prediction: a wavelet neural network approach, Expert Syst. Appl. 41 (9) (2014) 4422–4433.
[13] Y.M. Aung, A. Al-Jumaily, sEMG based ANN for shoulder angle prediction, Procedia Eng. 41 (2012) 1009–1015.
[14] T. Hayashi, H. Kawamoto, Y. Sankai, Control method of robot suit HAL working as operator's muscle using biological and dynamical information, IEEE/RSJ International Conference on Intelligent Robots and Systems, Edmonton, Alta (2005) 3063–3068.
[15] D.R. Rogers, D.T. MacIsaac, EMG-based muscle fatigue assessment during dynamic contractions using principal component analysis, J. Electromyogr. Kinesiol. 21 (5) (2011) 811–818.
[16] A.C. Tsai, J.J. Luh, T.T. Lin, et al., A comparison of upper-limb motion pattern recognition using EMG signals during dynamic and isometric muscle contractions, Biomed. Signal Process. Control 11 (2014) 17–26.
[17] G.E. Hinton, R.R. Salakhutdinov, Reducing the dimensionality of data with neural networks, Science 313 (2006) 504–507.
[18] H.J. Hermens, B. Freriks, C. Disselhorst-Klug, et al., Development of recommendations for SEMG sensors and sensor placement procedures, J. Electromyogr. Kinesiol. 10 (5) (2000) 361–374.
[19] V. Camomilla, A. Cereatti, G. Vannozzi, et al., An optimized protocol for hip joint centre determination using the functional method, J. Biomech. 39 (6) (2006) 1096–1106.
[20] M.E. Harrington, A.B. Zavatsky, S.E.M. Lawson, et al., Prediction of the hip joint centre in adults, children, and patients with cerebral palsy based on magnetic resonance imaging, J. Biomech. 40 (3) (2007) 595–602.
[21] C.L. Vaughan, B.L. Davis, J.C. O'connor, Dynamics of Human Gait, 2nd edition, Human Kinetics Publishers, Champaign Illinois, 1992, pp. 83–106.
[22] R. Sarikaya, G.E. Hinton, A. Deoras, Application of deep belief networks for natural language understanding, IEEE/ACM Trans. Audio Speech Lang. Process 22 (4) (2014) 778–784.
[23] S. Bu, Z. Liu, J. Han, J. Wu, et al., Learning high-level feature by deep belief networks for 3-D model retrieval and recognition, IEEE Trans. Multimedia 16 (8) (2014) 2154–2167.
[24] G.E. Hinton, A practical guide to training restricted Boltzmann machines, Momentum 9 (2012) 926.
[25] G.E. Hinton, Training products of experts by minimizing contrastive divergence, Neural Comput. 14 (8) (2002) 1771–1800.
[26] M.H. Schwartz, A. Rozumalski, J.P. Trost, The effect of walking speed on the gait of typically developing children, J. Biomech. 41 (2008) 1639–1650.
[27] V.L. Chester, M. Tingley, E.N. Biden, A comparison of kinetic gait parameters for 3–13 year olds, Clin. Biomech. 21 (2006) 726–732.